

Supplementary Information

Rapid Detection of Airborne Protein from *Mycobacterium tuberculosis* through a Biosensor Detection System

Jinbiao Ma ^{a, b, #}, Guanyu Jiang ^{a, b, #}, Qingqing Ma ^e, Hao Wang ^{c, f}, Manman Du
^{a, b}, Can Wang ^{a, b, *}, Xinwu Xie ^{c, d, *}, Tie Li ^{g, h}, Shixing Chen ^{g, h}

^a School of Environmental Science and Engineering, Tianjin University, Tianjin,
300072, PR China

^b Tianjin Key Lab of Indoor Air Environmental Quality Control, Tianjin, 300072, PR
China

^c Institute of Medical Support Technology, Academy of Military Science, Tianjin,
300161, PR China

^d National Bio-Protection Engineering Center, Tianjin, 300161, PR China

^e Department of Respiratory Medicine, Shandong public Health Clinical Center
(Shandong Province Chest Hospital), Jinan, 250013, PR China

^f School of Electronic Information and Automation, Tianjin University of Science and
Technology, Tianjin, 300222, PR China

^g Science and Technology on Micro-system Laboratory, Shanghai Institute of
Microsystem and Information Technology, Chinese Academy of Sciences, Shanghai
200050, PR China

^h State Key Laboratories of Transducer Technology, Shanghai Institute of Microsystem
and Information Technology, Chinese Academy of Sciences, Shanghai, 200050, PR

China

#These authors contributed equally to this work.

*Corresponding authors

E-mail addresses: wangcan@tju.edu.cn (Can Wang); xinwuxie@163.com (Xinwu Xie);

Content

Figure

1. Optimization of EBC acquisition parameters:

Figure S1. The establishment and practical application evaluation of the collection method of exhaled breath condensate.

Figure S2. Physical picture of optimization device for exhaled air acquisition conditions.

Figure S3. A physical view of an air sampling device for a volunteer's exhaled breath.

2. Biosensor detection system:

Figure S4. Changes in the hydrophilic angle of PMMA before and after modification of norepinephrine bitartrate monohydrate.

Figure S5. Physical diagram of automatic microfluidic detection system.

Figure S6. Gradient PBS solution test liquid path system.

3: Verification of biological activity.

Figure S7. Plate culture results in SEBC at different condensation temperatures.

Figure S8. The effect of condensing temperature on microbial activity in SEBC.

Figure S9. Optimization of condensing temperature and collection time.

4. Simulated air sample detection:

Figure S10. Physical diagram of simulated exhaled air sampling device.

Figure S11. Physical diagram of simulated aerosol sampling device.

Table

Table S1. The main non-biological components and concentration of SEBC

Table S2. The drag coefficient under different pipe diameters

Figure

1. Optimization of SEBC acquisition parameters:

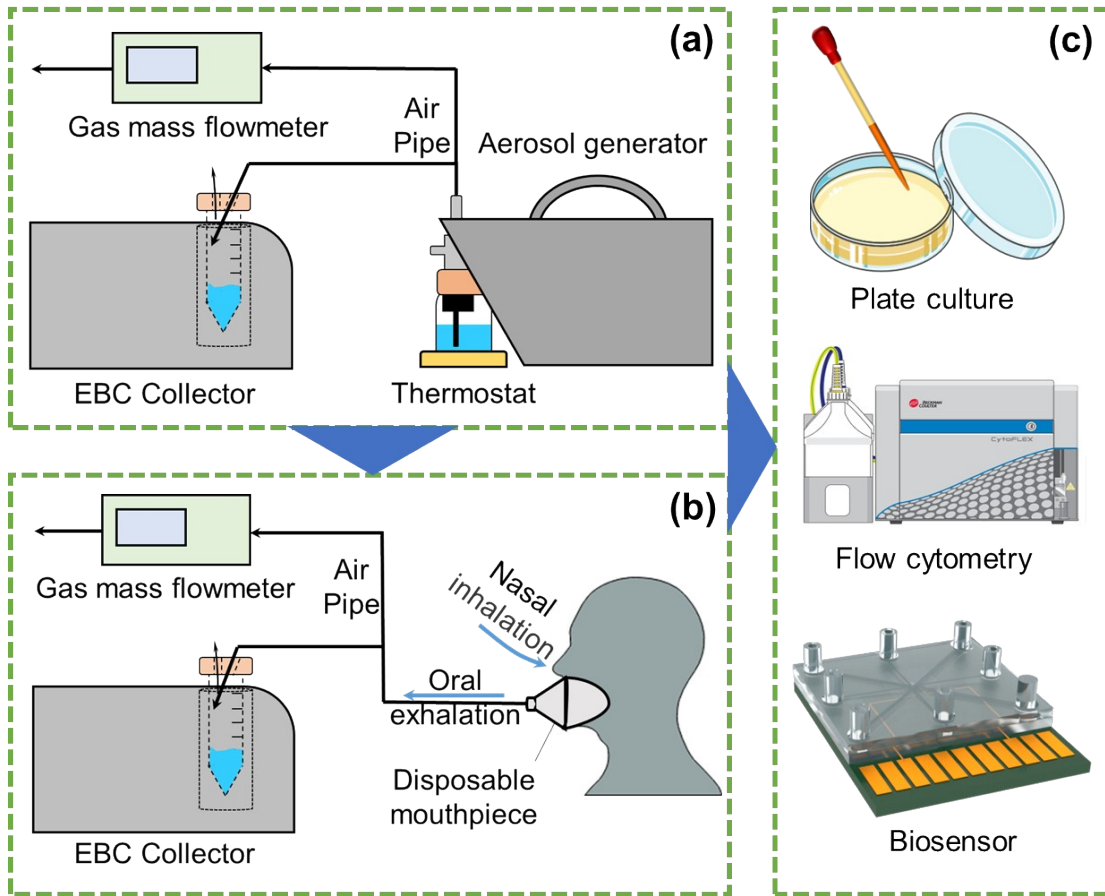


Figure S1. The establishment and practical application evaluation of the collection method of exhaled breath condensate. (a) The simulated exhaled breath output by the aerosol generator was collected by the SEBC condensate collector. (b) The exhaled aerosol of volunteers was directly collected by the EBC condensate collector. (c) Optimization of aerosol acquisition parameters and verification of microbial activity.

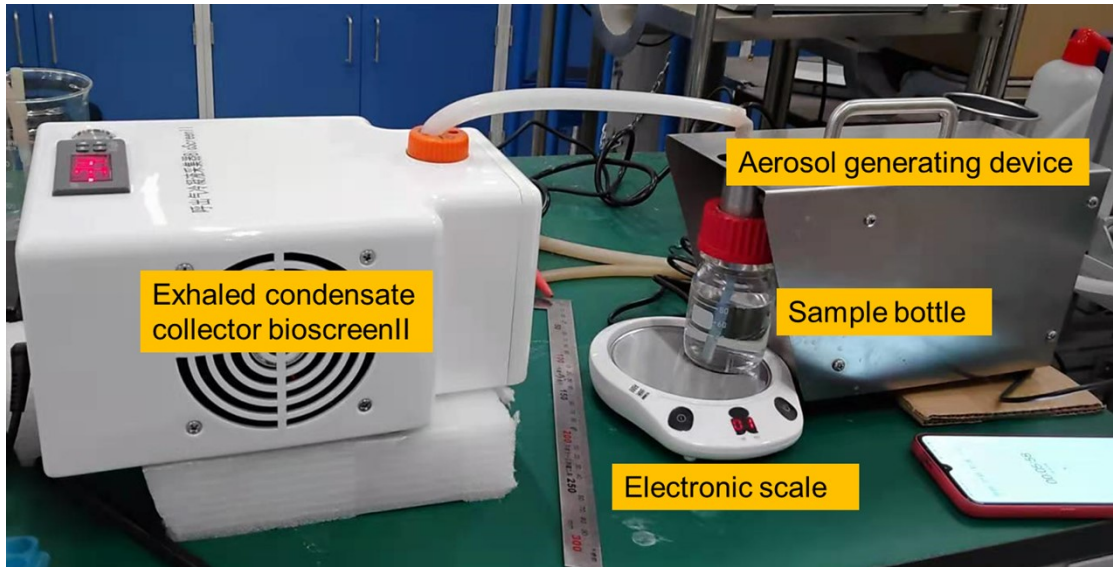


Figure S2. Physical picture of optimization device for exhaled air acquisition conditions.

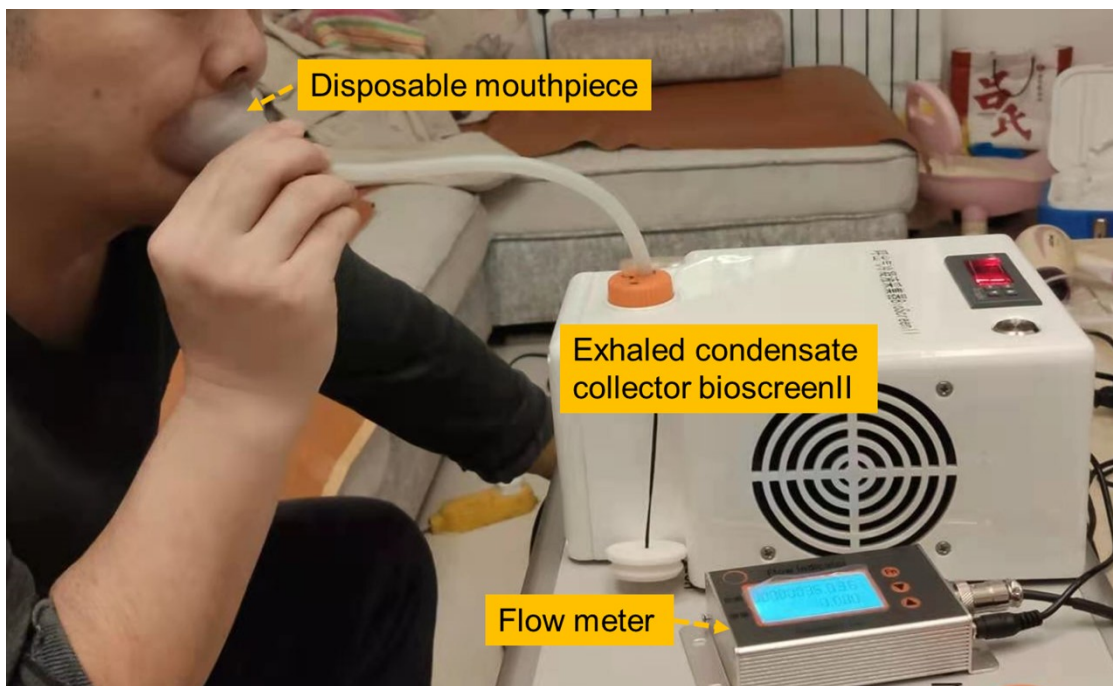


Figure S3. A physical view of an air sampling device for a volunteer's exhaled breath.

2. Biosensor detection system:



Figure S4. Changes in the hydrophilic angle of PMMA before and after modification of norepinephrine bitartrate monohydrate.

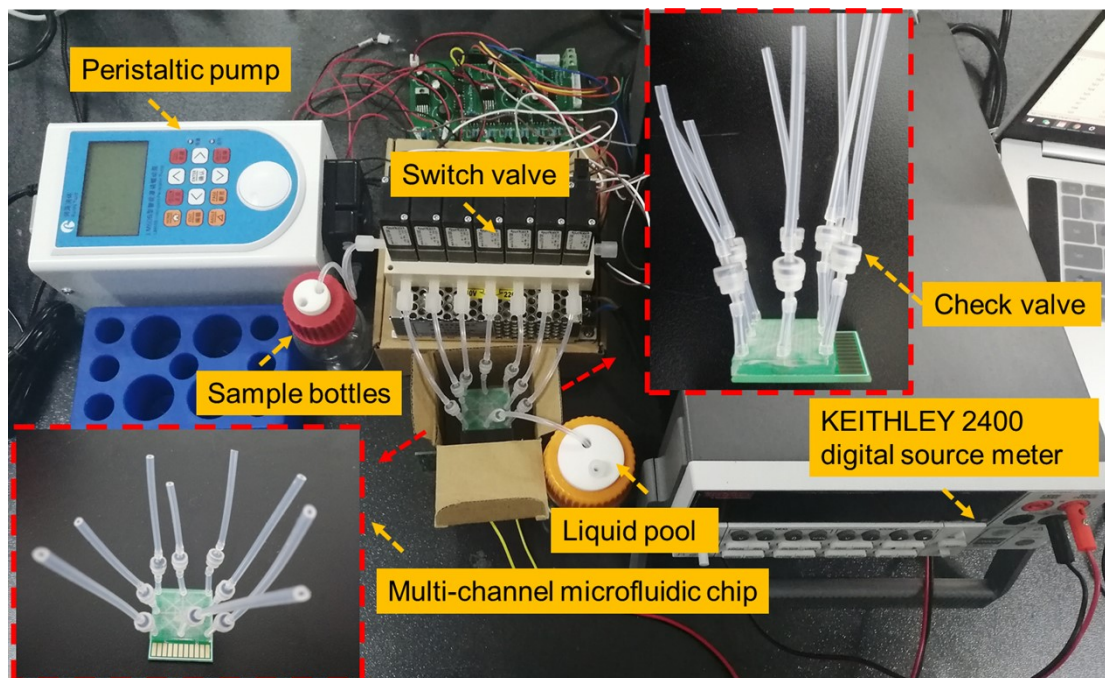


Figure S5. Physical diagram of automatic microfluidic detection system.

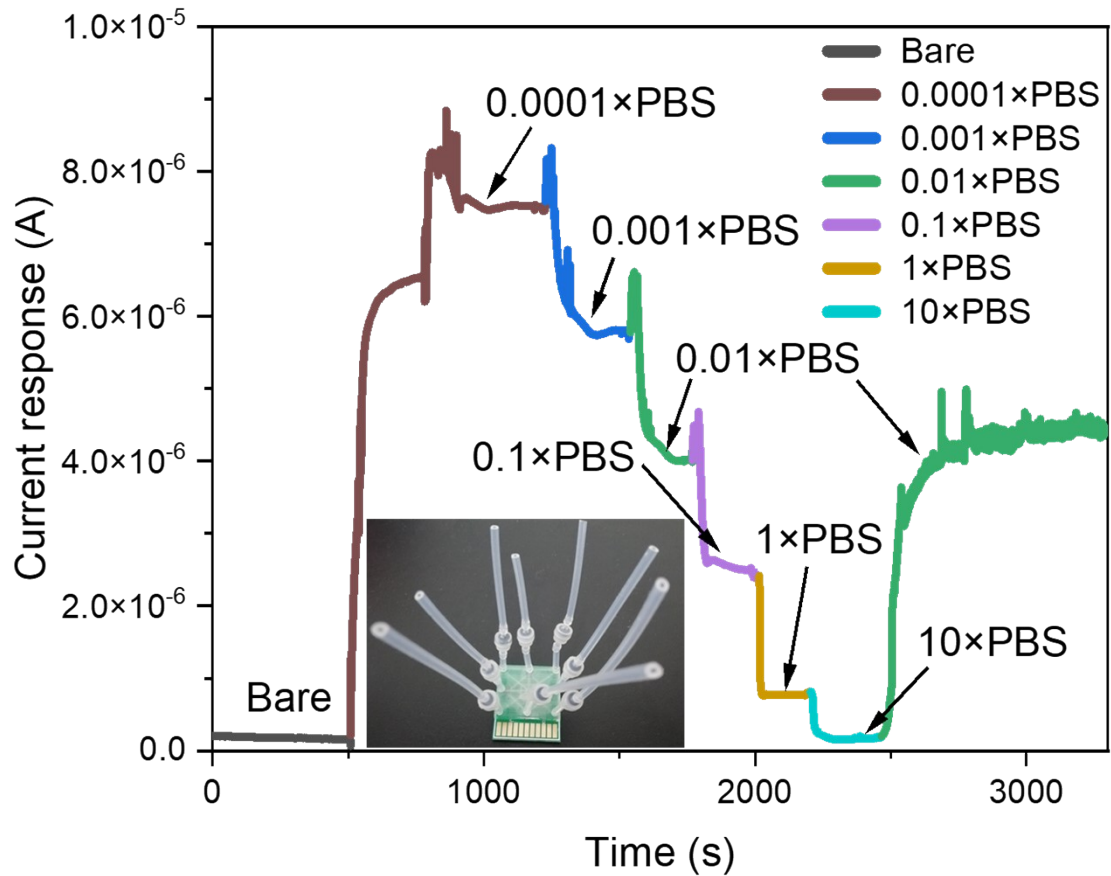


Figure S6. Gradient PBS solution test liquid path system.

3: Verification of biological activity.

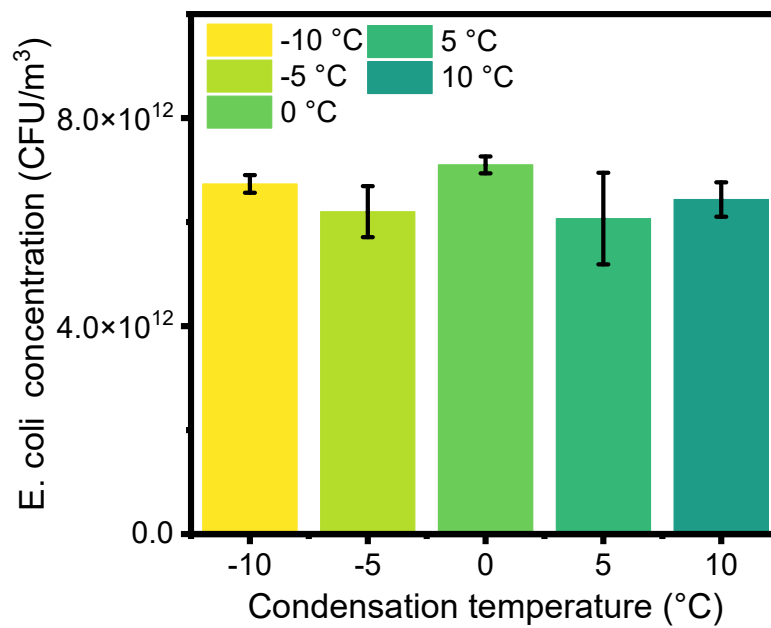


Figure S7. Plate culture results in SEBC at different condensation temperatures. Each data set displayed the average and SD of the results from three independent experiments (n= 3).

The flow cytometry analysis results of SEBC are shown in Figure S8(a)~(e). There is no significant difference in the survival status of *E. coli* at different condensation temperatures, which is consistent with the trend obtained by the plate culture method. The proportion of mechanically damaged cells was stable at 7%-8% under different condensation temperatures, indicating that the microbial loss during the sampling process is mainly a systematic error in the occurrence, transportation, and condensation processes. It has nothing to do with the condensation temperature. The proportion of living cells is stable at 77%~82%, while the proportion of living cells at 10 °C is slightly lower than other temperatures. This is because some living cells transform into early apoptotic cells in the in vitro environment. In flow cytometry staining, both living cells and early apoptotic cells can be regarded as cells with cellular structure. As shown in Figure S8(f), cells with cellular structure at different condensation temperatures account for 82% to 84% of stable cells. It also fully demonstrated the stability of the exhaled breath condensation collection method and its protective effect on microorganisms.

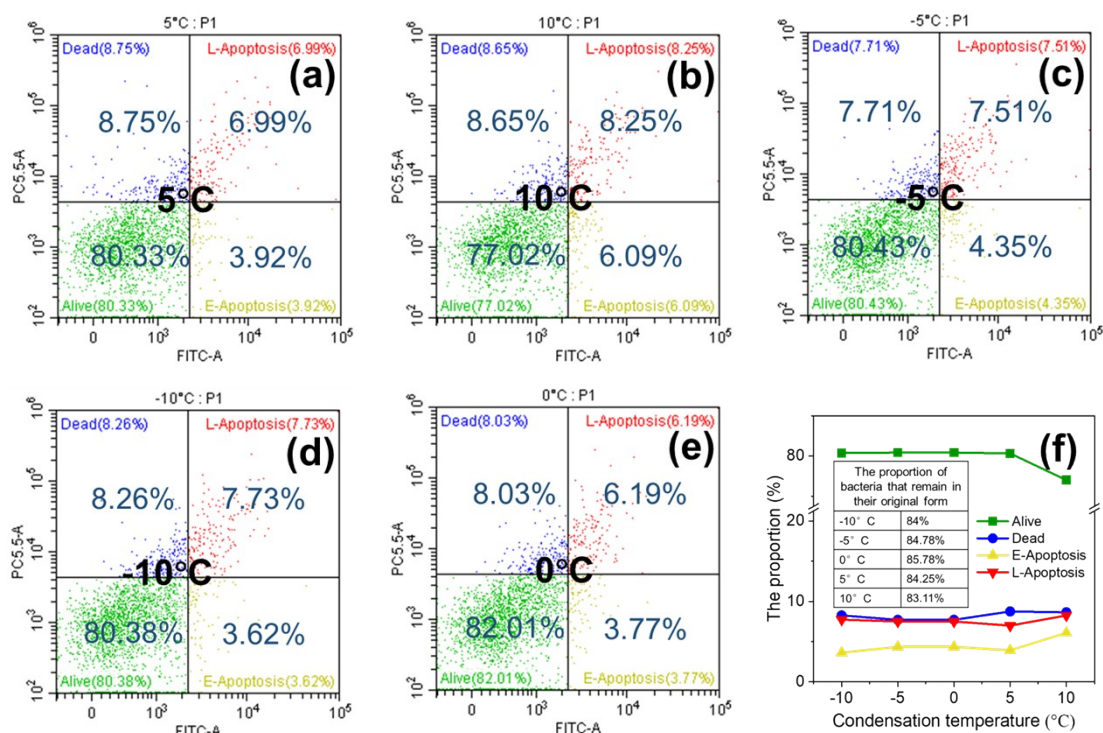


Figure S8. The effect of condensing temperature on microbial activity in SEBC. (a)~(e) The proportion of Escherichia coli activity was determined by flow cytometry at five different temperatures:

(a) 5°C, (b) 10°C, (c) -5°C, (d) -10°C, (e) 0°C. (living cells, Q5-LL, green), (mechanically damaged cells, Q5-UL, blue), (early apoptotic cell, Q5-LR, yellow), (late apoptotic cell, Q5-UR, red). (f) Quantitative results of cell state at different temperatures.

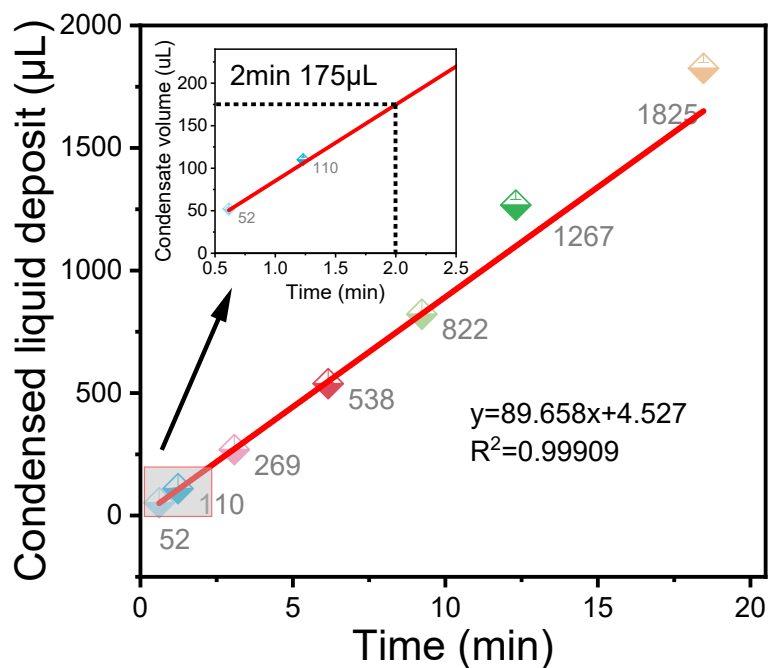


Figure S9. Optimization of condensing temperature and collection time. Linear fit between the collection time and the volume of SEBC at 0 degrees condensing temperature. Each data set displayed the average and SD of the results from three independent experiments (n= 3).

4. Simulated air sample detection:

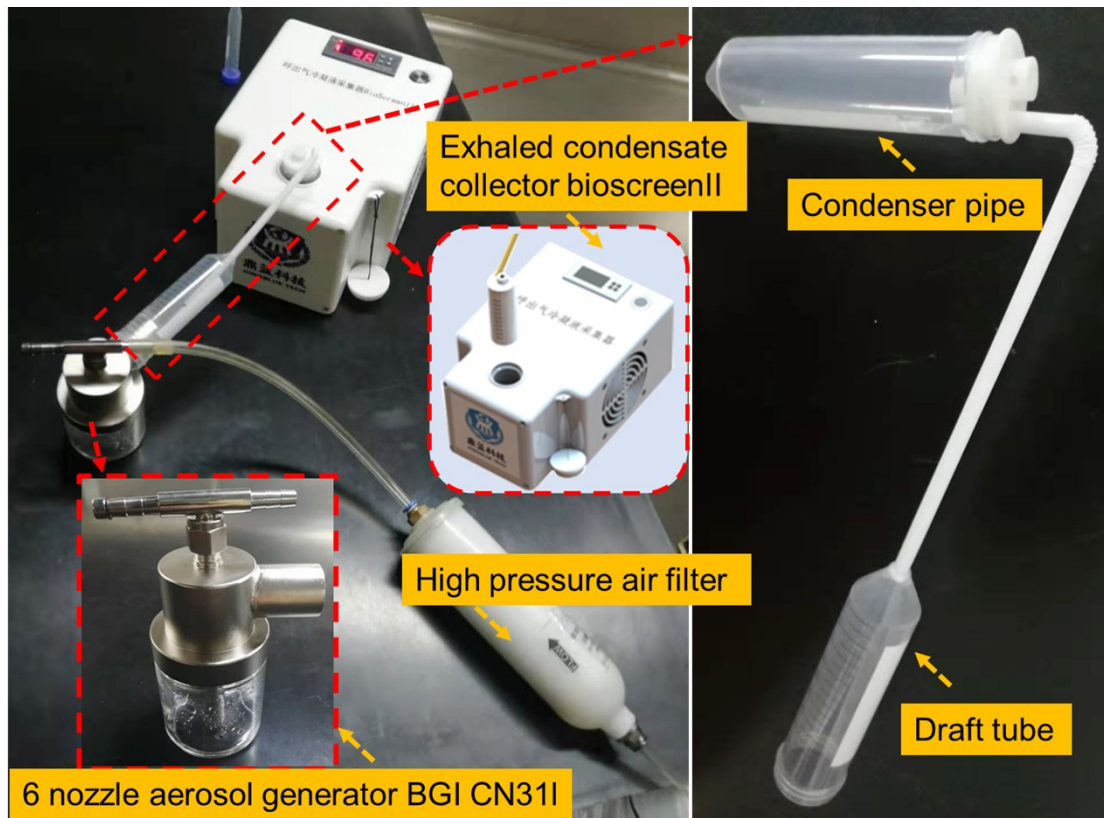


Figure S10. Physical diagram of simulated exhaled air sampling device.

For densely populated TB hotspots, the collection of exhaled breath appears to be inadequate. Intensive patients may release pathogens into the air when coughing, sneezing, breathing or even speaking. Since the diameter of the aerosol droplets produced by human exhalation is less than 100 μm , pathogens exhaled through the droplets may spread a considerable distance. In addition, some pathogens are atomized into the air from other body fluids (such as blood or feces). This will result in more TB in the air in hot spots of TB. Issues such as collecting, quantitatively analyzing and monitoring microorganisms in the air and determining relevant risk exposure thresholds need to be resolved urgently.

Then the outlet of the sprayer is connected to the air mixing barrel for aerosol simulation mixing (Figure S11), with a diameter of 30cm and a length of 150cm. The Coriolis Micro Bio-Aerosol Sampler was used to collect the aerosol at the outlet of the mixing barrel. The wind speed was 250l/min, the sampling time was 10min, and 5ml 0.01 \times PBS buffer was used for collection. It is continuously transmitted to the microfluidic chip through a peristaltic pump at a control flow rate

of 0.3 mL/min, and connected to the signal acquisition system for detection. The PBS buffer and 100ng/mL Ag85B protein were collected by aerosol simulation.

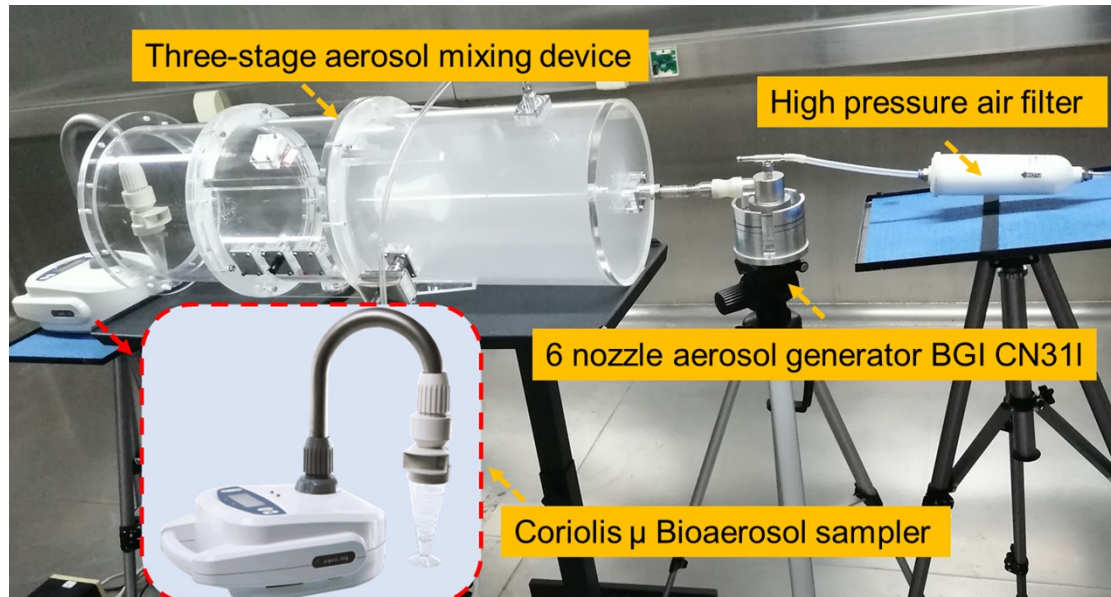


Figure S11. Physical diagram of simulated aerosol sampling device.

Table

SEBC is mainly composed of water and respiratory tract lining fluid, most of which are water, and respiratory tract lining fluid only accounts for 0.01% to 2% of SEBC. Table S1 shows the main non-biological components and their concentrations that affect the physical and chemical properties of SEBC. This experiment simulates the actual SEBC of human body by adding salt, acid and macromolecular protein with a certain proportion into the sterile deionized water. According to the concentration, we add 0.0123 g ammonium chloride, 0.014 g sodium chloride, 0.0059 g potassium chloride, 32.6 μ L lactic acid and 0.023 g bovine serum albumin to 1 L of deionized water.

Table S1. The main non-biological components and concentration of SEBC

Composition	Concentration (μ mol/L)
NH_4^+	229 \pm 49
Na^+	242 \pm 140
K^+	80 \pm 36
Cl^-	231 \pm 109
Lactic acid	393 \pm 305
Protein	2.3 mg/L

Table S2. The drag coefficient under different pipe diameters

Pipe diameter (mm)	2	4	5	6	8
Flow velocity, (m/s)	22.8	5.7	3.64	2.53	1.42
Drag coefficient	0.03791	0.03791	0.03791	0.03791	0.03861

Under the conditions of known pipe material, pipe length L , pipe diameter D , fluid density ρ , fluid viscosity μ , and pipeline flow Q , the drag coefficient in the pipe can be calculated by software Pipedrop1.2.3.